Reply to Referee #1

General comment

> *This manuscript presents a temperature uncertainty characterization of the FrESH droplet-freezing assay. Accurate temperature assignment is undoubtedly important for offline measurements of ice-nucleating particles. The authors have also performed a careful set of static and dynamic temperature measurements and constructed an uncertainty budget for the instrument.*
> *However, I have a major concern regarding the novelty and scientific contribution of the present manuscript. In its current form, the work is largely limited to temperature characterization of a specific droplet-freezing instrument. This is primarily an instrumental and engineering characterization problem. I do not see a sufficiently substantial technical innovation or scientific advance that would justify publication as a standalone study. A substantially stronger manuscript would require additional experimental content. In particular, an intercomparison with an established instrument and/or a scientific application demonstrating the benefit of the improved temperature characterization would considerably strengthen the work. Therefore, I cannot recommend publication in its present form.*

We thank the referee for the evaluation. It motivated us to conduct additional experiments to strengthen the revised manuscript, in addition to the more than 1,000 experiments conducted for the characterisation. With the additional experiments, we tested the position-dependent freezing pattern using relocated PT100 sensors and repeated measurements of the same droplets after rotating and transferring their plates. We also investigated the effect of cooling rate and added an ambient INP-spectrum example showing the effect of the bath-to-well correction and temperature uncertainty. The additional measurements highlight how characterising a droplet-freezing setup using the methods presented here can benefit the interpretation of scientific questions, such as the cooling-rate dependence of freezing and the interpretation of temperature-cycling experiments. They help assess the contribution of experimental variations before attributing observed changes to the underlying freezing behaviour, while also showing the limits of this separation.

For a comparison with an established instrument, we reprocessed the FrESH measurements from the six-filter intercomparison with GRAINS reported by Bazo et al. (2026). This shows the effect of the bath-to-well correction derived here (RC1-3). We refer to that publication for the full intercomparison, which also includes comparisons of GRAINS with INSEKT and PINE.

We reply to the specific comments below, stating:

What we did and why.

What we found.

Changes in the revised manuscript.

RC1-1

> *The main result is an operational droplet-temperature uncertainty of approximately 0.43–0.44 °C. This is useful for FrESH measurements, but it is not clear what is fundamentally new compared with previous droplet-freezing instruments. The reported uncertainty of FrESH is somewhat smaller than that of some instruments (Table 3). The authors should therefore explain much more*

> *clearly what technical development in FrESH leads to improved temperature accuracy. At present, I mainly see a careful calibration procedure rather than a clear technical innovation.*

The main contribution of this study is the development and demonstration of a systematic framework for characterising droplet-temperature assignment and quantifying its associated uncertainty, supported by an extensive experimental dataset. The benefit for the INP measurement community is a more reliable temperature assignment, together with a transparent and reproducible approach to quantifying and reporting its uncertainty. We now make this distinction more explicit in the revised manuscript. Additionally, we investigate the possible reasons why uncertainty budget characterization of similar drop freezing setups differ between studies.

What we did and why.

We checked how each value in Table 3 was derived in the cited studies, to see whether the values can be compared, and revised Table 3 accordingly (Table R1). The value for FrESH is updated to 0.44–0.50 °C with the revised spatial term (0.43–0.44 °C in the submitted manuscript; RC1-2).

What we found.

The reported values differ in their definitions, experimental procedures, uncertainty contributions and combination methods (Table R1). For example, FINC reports the spread of temperature measurements across selected wells, micro-PINGUIN reports an expanded uncertainty ($k = 2$, where k is the coverage factor multiplying the combined standard uncertainty), and FINDA-WLU, DRINCZ and TINA linearly add their contributions. FrESH reports a combined standard uncertainty ($k = 1$), with its contributions added in quadrature and the spatial variability kept as a term of the budget rather than corrected well by well (RC1-2). Because of these methodological differences, the reported values do not rank instrument accuracy; they mainly reflect how each value is defined and which contributions it includes.

Within FrESH, the bath-to-well correction addresses the systematic difference between the recorded bath temperature and the estimated well temperature. According to the fitted bath-to-well relations (Table 1), the estimated well temperatures are approximately 0.2 to 1.3 °C warmer than the bath over the range from 0 to −35 °C. Using the bath temperature directly would therefore assign systematically colder freezing temperatures. The uncertainty budget describes the remaining uncertainty in the corrected assignment.

Changes in the revised manuscript.

We do not claim a technical development that makes FrESH more accurate than other instruments; the contribution is the method for characterising the droplet-temperature assignment and quantifying its uncertainty. The Introduction and Conclusions now state this explicitly, citing the precedents for position maps derived from freezing statistics (David et al., 2019; Kunert et al., 2018). Table 3 is replaced by Table R1, which states what each reported value represents and which contributions it includes, and Sect. 5 explains that these values therefore do not rank instrument accuracy. The bath-to-well correction is described as removing a systematic offset within FrESH relative to the recorded bath temperature, not as an improvement over other instruments.

Table R1. Revised Table 3: reported temperature-characterisation values, with what each value represents and which contributions it includes.

Instrument	Reported value	What the value is	Contributions included
FrESH (this work)	0.44–0.50 °C	Combined standard uncertainty ($k = 1$), terms added in quadrature	Bath probe, bath-to-well relation, temporal resolution, spatial and dynamic terms
FINC (Miller et al., 2021)	±0.5 °C	Mean standard deviation of nine thermocouples in ethanol-filled wells in three trays	Differences between wells, down to −25 °C at 1 °C min^{-1}
FINDA-WLU (Wang et al., 2025)	±0.60 °C	Linear sum; regression terms taken as twice their standard deviation	PT100 calibration, infrared-camera calibration, per-well horizontal calibration, sensor accuracy, camera
GRAINS (Bazo et al., 2026)	<0.5 °C	Propagated uncertainty	PT100 probe; block-to-well correction from orthogonal distance regression
DRINCZ (David et al., 2019)	±0.9 °C	Linear sum, described as an upper limit on instrumental precision	Calibration (±0.6 °C, the largest standard deviation of well temperatures about the bath-to-well fit); pure-water freezing repeatability (±0.3 °C)
micro-PINGUIN (Wieber et al., 2024)	±0.81 °C	Expanded uncertainty ($k = 2$) at −10 °C	Temperature-dependent combined standard uncertainty, dominated by the vertical temperature gradient in the well
TINA (Kunert et al., 2018)	<0.2 °C	Linear sum, after a well-by-well correction	Thermistor calibration, thermocouple measurement, residual standard deviation of fungal-filtrate freezing temperatures after the correction derived with the same filtrate

RC1-2

> *One of the larger contributions to the total uncertainty is the spatial term. However, this term is inferred from position-dependent freezing patterns observed over routine measurements, rather than from direct temperature measurements across the 96 wells.*

Referee #2 raised the same concern (RC2-1). In response, we re-examined the routine runs used to derive the c_i field and carried out two additional experiments: direct PT100 measurements in selected wells, and repeated freezing measurements of the same droplets after rotating or transferring their plates between instrument positions.

What we did and why.

Refined determination of the c_i field. The c_i field is derived from routine measurements. For each well, c_i is the mean difference between its freezing temperature and its plate's median, calculated using the recorded bath temperature. The spatial uncertainty contribution u_{spatial} is the standard deviation of c_i over the 96 wells, each well weighted by the number of plates in which it has a value, using the larger value of the two plate positions in each chiller. In preparing this response we re-checked which routine runs belong to each chiller and plate position. The submitted field had included runs from an earlier chiller and from blank samples, and part of the plates had been read with the wells in the opposite order; this affected only the analyses of individual wells, not the INP spectra. The rebuilt field (Fig. R1) keeps its

shape (correlation with the submitted one 0.88–0.96). Its standard deviation is 0.26 and 0.36 °C for plate positions A and B of the RE1050 and 0.36 and 0.29 °C for those of the RP1845 (351, 343, 499 and 501 plates; 0.20, 0.26, 0.36 and 0.23 °C in the submitted field), so that u_{spatial} is now 0.36 °C for both chillers (0.26 and 0.36 °C in the submitted manuscript). The calibration coefficients a and b come from the static step runs (Table A1) and are not affected. All analyses below use the revised field.

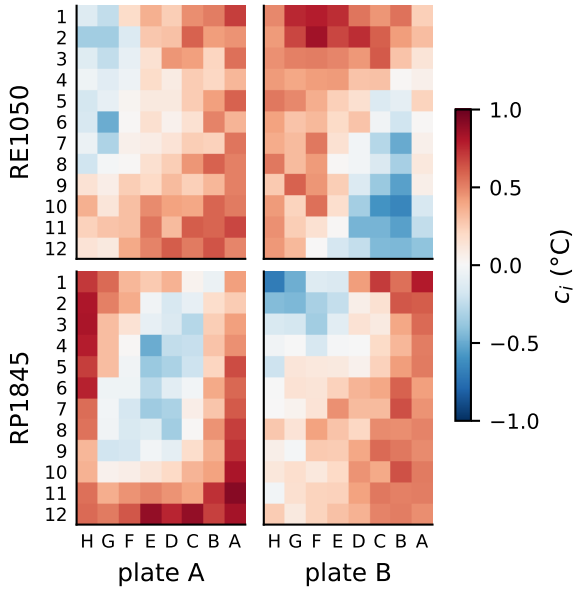


Figure R1. The c_i field of each plate position, revised. The plates are drawn as they sit in the bath, plate A to the left of plate B. Colour: the mean offset of a droplet's freezing temperature from its plate's median, on the bath temperature (positive: the droplet freezes at a warmer bath temperature).

Additional cycling experiments. Four PCR plates were filled once and then frozen and thawed repeatedly; we call them the fixed plates. They were two replicate plates of the same ambient filter suspension (P1 and P2), a 1:10 dilution of it (P1_D10) and a water blank (WB). Each plate has a home position, the chiller and plate position where it was first measured. Each plate was measured at its home position at 1 °C min^{-1} and rotated by 180° there, in September and again in October (in September, P1_D10 and WB were instead taken out and put back unrotated, as a handling control). It was then measured in the same plate position of the other chiller, in the other plate position of the other chiller, in the other plate position of its own chiller, and again at home. The more than 100 cycles per plate are listed in Table R2. Tracking the same droplets through these changes tests whether differences in assigned freezing temperature are associated with the plate or with its position in the holder. The plates were kept frozen between measurement sessions.

Additional PT100 measurements. We used direct temperature measurements to test whether wells with contrasting values of c_i also differed in temperature during cooling. Five PT100 sensors were placed in wells containing 50 µL of Milli-Q water each. One sensor remained in well A6 of plate position A as a reference. The other four were moved between runs to selected edge and interior wells (Fig. R2). The positions were selected using the submitted field; the comparisons below use the revised one.

The sensors were checked together in a Milli-Q ice–water bath and in a stirred ethanol bath at setpoints from 0 °C to −35 °C, alongside a reference thermometer (Lufft XP100). The ethanol-

Table R2. The cycling experiment at 1 °C min^{-1}: where each plate was at each step, its orientation, and the number of cycles analysed (the first cycle of each run left out). *: the step in which the plate changed, and the steps after it; not used.

Step	P1	P2	P1_D10 (1:10)	WB (water)
Home	RE1050 A, 0° (24)	RP1845 A, 0° (22)	RE1050 B, 0° (24)	RP1845 B, 0° (22)
Home, rotated[a]	RE1050 A, 180° (24)	RP1845 A, 180° (26)	RE1050 B, 0° (24)	RP1845 B, 0° (26)
Home	RE1050 A, 0° (7)	RP1845 A, 0° (7)	RE1050 B, 0° (7)	RP1845 B, 0° (7)
Home, rotated	RE1050 A, 180° (19)	RP1845 A, 180° (9)	RE1050 B, 180° (19)	RP1845 B, 180° (18)
Other chiller, same position	RP1845 A, 180° (6)	RE1050 A, 180° (6)	RP1845 B, 180° (6)	RE1050 B, 180° (6)
Other chiller, other position	RP1845 B, 180° (17)*	RE1050 B, 180° (16)	RP1845 A, 180° (17)	RE1050 A, 180° (16)
Same chiller, other position	RE1050 B, 180° (6)*	RP1845 B, 180° (5)*	RE1050 A, 180° (6)	RP1845 A, 180° (5)
Home	RE1050 A, 0° (17)*	RP1845 A, 0° (16)*	RE1050 B, 0° (17)	RP1845 B, 0° (16)
All cycles at 1 °C min^{-1}[b]	141	113	124	116

[a]P1_D10 and WB were taken out and put back unrotated, as a handling control. [b]Including single ramps and short series at the home position.

bath measurements were used to correct temperature-dependent offsets between sensors.

We used the ramps at the routine 1 °C min^{-1}. For each relocated sensor we took its temperature minus that of the reference sensor while the water around both was still liquid and the bath was between −10 °C and −18 °C, the range in which about three quarters of the routine droplets behind c_i froze, and averaged it over the ramps of the run. This gives one temperature difference per sensor and run, which we call a placement.

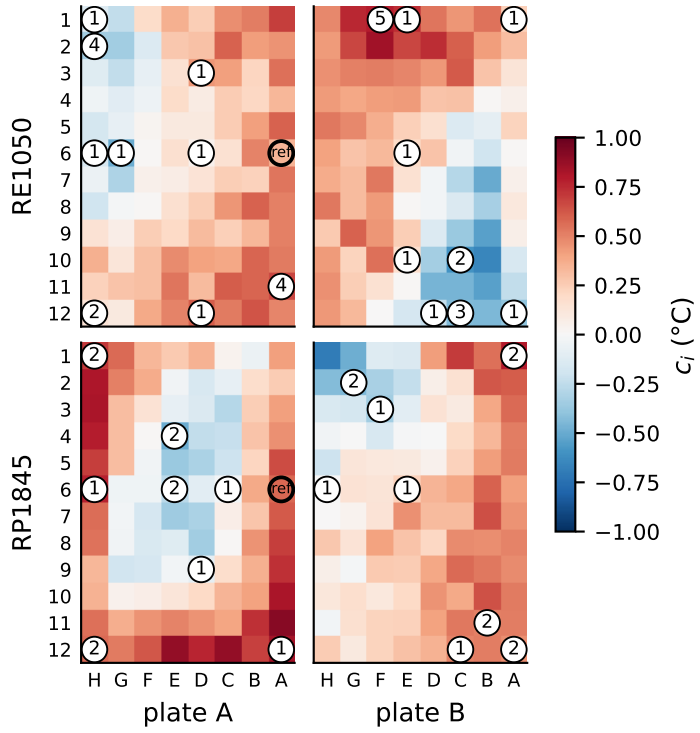


Figure R2. The wells measured with the PT100 sensors, on the c_i field of each plate position: the number of runs in each well; ringed, the reference sensor in A6 of plate A.

What we found.

The c_i field predicts how the assigned freezing temperature of a droplet should change when it is moved from one well position to another: by c_i at the new position minus c_i at the old one. We compared the measured changes with this prediction.

The fixed-plate experiments test whether instrument position contributes to the routine freezing pattern. If the c_i field captures this contribution, moving the same droplets should change their assigned freezing temperatures in the direction predicted by the field. Comparing each droplet with itself controls for persistent differences in freezing behaviour between droplets.

For the rotations, we compared opposite well pairs. Taking half the difference between their measured changes removes a shift common to the plate and estimates the difference between the two positions, $F(p) - F(p')$. We fitted these measured differences against those predicted by the c_i field, $c_i(p) - c_i(p')$ (Fig. R3a for P1; Table R3). For example, the field predicts a difference of 1.02 °C between wells A11 and H2; rotating P1 gave 0.79 °C (ringed in Fig. R3a). As a handling control, taking P1_D10 and WB out and putting them back unrotated gave no position effect (slopes of -0.02 and 0.10, against 0.79 for the first rotation of P1).

The fitted slopes were 0.82 and 0.52 for the two undiluted replicate plates, P1 and P2, 0.32 for the 1:10 dilution, and 0.02 (-0.22–0.22) for the water blank, i.e. no detectable effect; a slope of 1 would indicate agreement in magnitude. P2's slope was less constrained because its home-position field was nearly symmetric under rotation, giving smaller predicted contrasts. The undiluted plates froze in the range of the routine plates (plate medians of about -13.5 °C, against about -15 °C for the routine plates in all four plate positions), the dilution about 6 and the blank about 15 °C colder. Freezing range and plate position cannot be separated here: both undiluted plates were in plate position A and the dilution and blank in B, and P1 and P2 were on different chillers. The blank's null result is not what a purely thermal field would give, since the temperature differences between wells grow as the bath cools (RC2-4); it suggests that the field is not purely thermal, or that it changes below about -20 °C, where the baths no longer follow 1 °C min^{-1}.

Transfers between chillers and plate positions gave a similar result. For row-averaged changes, the measured changes were positively correlated with the predicted pattern in 8 of the 9 transfers made before a plate's freezing pattern changed ($r = 0.42$–0.91 over the eight holder rows; the 95 % interval excludes zero in five of them), with fitted slopes of 0.2–1.0. The exception was a water-blank transfer for which the predicted contrast between rows was small. Agreement was weaker for individual droplets: their changes between repeated runs at the same position were comparable to the changes associated with transfers.

As a sensitivity test, we repeated the rotation analysis using pairs selected for stable freezing temperatures at their home position. The slopes for P1 and P2 increased to 0.94 and 0.92, with wider intervals. These were at the 76th and 84th percentiles of slopes from 20 000 random subsets of the same size (Table R3), so the increase towards 1 was not unusual among random subsets of the same size.

In summary, instrument position contributes to the routine freezing pattern: moving the same droplets generally changed their assigned freezing temperatures in the predicted direction, but usually by a smaller amount. These results support a position-dependent interpretation of part of the c_i field, but do not validate its full magnitude. The direct PT100 measurements below test whether the field corresponds to measured temperature differences between wells.

Direct PT100 measurements at selected wells showed temperature differences with the sign predicted by the c_i field, but smaller in magnitude (Fig. R3b). The fitted slopes (k) of measured

Table R3. Rotations in place: slope of the measured position differences against those predicted by the c_i field, a plate's rotations together, for all valid pairs and for the stability-selected pairs. Intervals are 95 %, from resampling the pairs. Pct.: percentile of the stability-selected slope among 20 000 random subsets with the same number of pairs.

			All valid pairs		Stability-selected pairs		
Plate	Position	Rotations	Pairs	Slope	Pairs	Slope	Pct.
P1	RE1050 A	2	48	0.82 (0.67–1.02)	12	0.94 (0.64–1.46)	76
P2	RP1845 A	2	47	0.52 (0.14–1.02)	15	0.92 (0.23–2.77)	84
P1_D10	RE1050 B	1	48	0.32 (0.14–0.50)	16	0.22 (0.06–0.41)	21
WB	RP1845 B	1	48	0.02 (-0.22–0.22)	13	0.26 (-0.01–0.53)	92

against predicted differences were 0.29 for the RE1050 (95 % interval 0.23–0.35; 32 placements in 8 runs) and 0.39 for the RP1845 (0.08–0.78; 22 placements in 6 runs), where a slope of 1 indicates agreement in magnitude. The measured temperature differences, about a third of those predicted, therefore do not fully explain the routine freezing pattern.

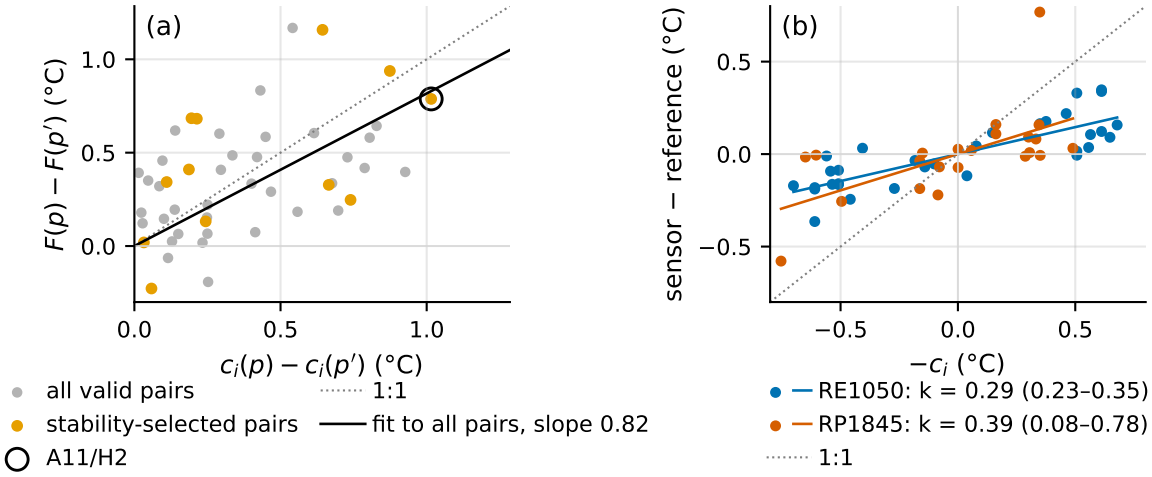


Figure R3. (a) Rotations of P1: for each pair of opposite positions, the measured difference between the two positions, $F(p) - F(p')$ (mean of the two rotations), against that predicted by the c_i field. (b) PT100 placements, liquid water, bath between −18 °C and −10 °C: temperature difference from the reference sensor against $-c_i$, after removing the run offsets and the plate-position offset of the fit. Panel (a) compares freezing temperatures and panel (b) measured temperatures, from different experiments.

The two experiments support a position-dependent contribution to the routine freezing pattern, but do not establish its full thermal origin. Rotating and transferring the same droplets changed their assigned freezing temperatures in the direction predicted by the c_i field, with magnitudes that varied between plates. Direct PT100 measurements also showed temperature differences with the expected sign, but smaller than those inferred from the field.

The discrepancy remains unresolved. On the RE1050, the part of the field that the measured temperatures do not explain still follows the position (rotation slope 0.82, against $k = 0.29$), so it cannot be an effect of the filling order or of the sample, which would travel with the droplets. Possible contributions include perturbation of the well temperature by the sensors and their leads, differences in sensor placement and thermal contact, and position-dependent optical detection. These measurements do not distinguish between these explanations.

The c_i field does not necessarily represent the spatial variability in every run. Therefore we do not interpret the c_i field as a temperature map, and we do not use it for well-specific corrections and keep the spatial term in the uncertainty budget as an operational estimate of the position-dependent variability of the assigned freezing temperature, not as a measured temperature difference. From the revised field, $u_{\mathrm{spatial}} = 0.36\,^{\circ}\mathrm{C}$ for both chillers. This raises the combined uncertainty of the RE1050 from 0.43 to 0.50 °C and leaves that of the RP1845 at 0.44 °C.

Other effects could influence the c_i field obtained from routine measurements. Any effect of the filling order, which is a real difference between droplets, would appear in the routine field as a position effect and could make the full term overestimate instrument-position variability (RC2-3). In the fixed plates, the rotation separates the two: for P1, the slope of 0.82 (0.67–1.02) leaves room for at most about a third of the rotation-sensitive part of the field to travel with the droplets.

Changes in the revised manuscript.

To address this comment, we added two tests that do not rely on the routine freezing statistics. New Methods subsections describe the cycling experiment with the fixed plates, including the handling control and the sensitivity test with stable droplets, and the relocated PT100 sensors (Fig. R2). A new Results section shows that moving the same droplets changes their freezing temperatures in the direction predicted by the c_i field, but usually by less, and that the directly measured temperature differences between wells are about a third of those predicted (Fig. R3, Table R3). The c_i field is rebuilt from each chiller's own routine plates (Sect. 3.2, Fig. 3). Sect. 4.3 and Table 2 now describe the spatial term as an operational estimate of the position-dependent variability of the assigned freezing temperature, partly explained by temperature differences between wells, and state its limitations, including the change of the field between periods of routine operation; the field is not used as a well-specific correction. The Abstract and Conclusions are revised accordingly, and the new data are added to version 2 of the dataset.

RC1-3

> *A direct comparison with other well-established immersion-freezing instruments would substantially strengthen the paper.*

FrESH participated in an intercomparison with GRAINS reported by Bazo et al. (2026). Six filters were divided in half, with one half analysed by each instrument. In the same study, GRAINS was also compared with the KIT instrument INSEKT and with PINE. The FrESH spectra in that study were assigned to the bath temperature, without the bath-to-well correction derived here, and Bazo et al. (2026) noted that the temperature shift between the two instruments could be due to this.

What we did and why.

We reprocessed the FrESH halves of the six filters with the current pipeline and assigned their freezing temperatures both to the bath temperature and to the droplet temperature from the relations derived here. Four of the filters had been measured on the RP1845. The other two had been measured on a third chiller (RK20), which is not characterised in this study; for these, we estimated the droplet temperature with the mean of the two characterised relations, which differ by about 0.1 °C at −15 °C. Because the RK20 itself was not characterised, this estimate is more uncertain than the corrections of the characterised chillers, which still differed by about

0.3 °C after correction (RC2-6).

What we found. For the four filters measured on the RP1845, the median difference from GRAINS at equal INP concentration was 1.6 °C on the bath temperature and 0.9 °C on the droplet temperature, FrESH being colder (Fig. R4). The correction therefore reduces the difference by about 0.7 °C, in the direction expected. Reprocessing alone already placed the bath-temperature spectra closer to GRAINS than the published ones (median difference 1.9 °C), so the effect of the correction is evaluated on the same reprocessed plates.

The remaining difference is of the order of the combined temperature uncertainty of the two instruments (0.44 °C for FrESH on the RP1845 and below 0.5 °C for GRAINS; shaded in Fig. R4), within which the spectra of two of the four filters agree. It may also reflect other differences between the two setups discussed by Bazo et al. (2026), such as the droplet volume (50 µL in FrESH, 100 µL in GRAINS). For the two filters measured on the RK20, the difference was 1.6 and 2.6 °C on the bath temperature, and 0.8 and 1.9 °C with the estimated droplet temperature. In addition, FrESH recently participated in a larger instrument intercomparison within ACTRIS, for which a paper is in preparation.

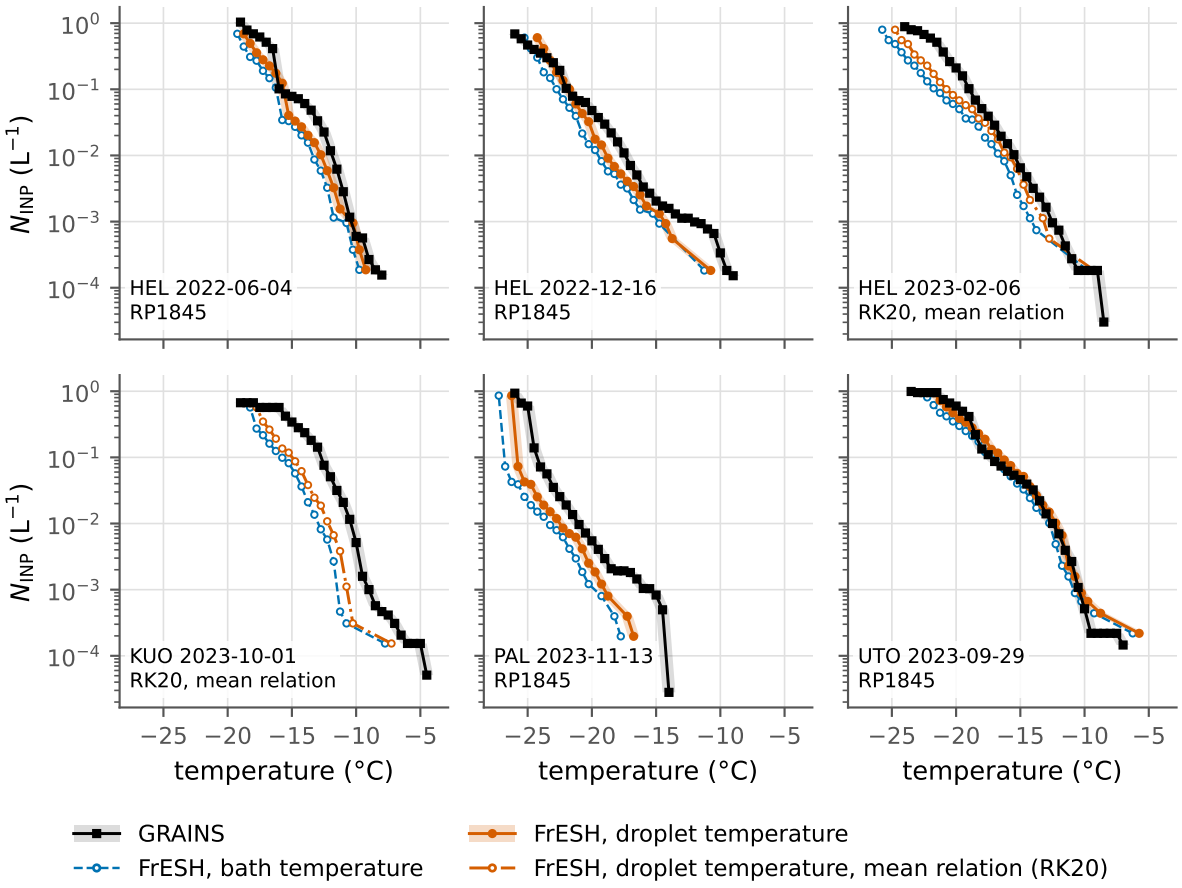


Figure R4. INP spectra of the six filters shared by FrESH and GRAINS (Bazo et al., 2026).

Changes in the revised manuscript.

A new section compares FrESH with GRAINS on the six filters shared in the intercomparison of Bazo et al. (2026), with the FrESH spectra assigned to the bath and to the droplet temperature (Fig. R4). The bath-to-well correction reduces the difference from GRAINS by about 0.7 °C,

to a remaining difference of the order of the combined temperature uncertainty of the two instruments. We refer to Bazo et al. (2026) for the full intercomparison.

RC1-4

> *Last but not least, the manuscript currently lacks a scientific application that demonstrates why this improved characterization matters.*

Schrod and Bingemer (2025) recently elucidated why the uncertainty of the activation temperature matters. INP activation is highly sensitive to temperature, and small activation-temperature errors can cause large over- or underestimates of INP concentration. They show that opposite biases of $\pm 0.5\,^{\circ}\mathrm{C}$ between instruments typically correspond to a factor of about 2 in INP concentration, and of $\pm 1\,^{\circ}\mathrm{C}$ to a factor of up to 5–10, so that such uncertainties must be carefully assessed and reported. In addition, how well temperature-cycling experiments can isolate the stochastic contribution to a droplet's freezing probability depends on the uncertainty in droplet temperature.

What we did and why.

To demonstrate its effect on a routine measurement, we calculated the $N_{\mathrm{INP}}(T)$ spectrum of an ambient filter from Pallas (25 August 2025, the suspension of the cycling experiment) from one freezing cycle of its undiluted and 1:10 plates on the RE1050, using the bath temperature and the bath-to-well correction. We used only the range where the spectrum is neither saturated nor reached by the water blank of the same run. To express the effect of a temperature difference on the concentration at a given temperature, we used the local slope s of the spectrum, in decades per °C: a temperature error δT changes the inferred concentration by a factor $10^{s\,\delta T}$ (Schrod and Bingemer, 2025).

What we found.

The correction shifts the spectrum by 0.61 to 0.89 °C over its range (Table 1). Assigning the bath temperature instead would underestimate the concentration at a given temperature by a factor of 1.37 (median; 1.2 to 2.6), most where the spectrum is steepest, at its warm end (Fig. R5). The temperature uncertainty of the RE1050, $u_T = 0.50\,^{\circ}\mathrm{C}$, corresponds to a factor of 1.21 in concentration (median; 1.14 to 2.0), for a median local slope of 0.17 decades per °C. For this spectrum, the effect of the correction is therefore larger than the remaining uncertainty. In the intercomparison (RC1-3), the same correction reduces the difference from GRAINS by about 0.7 °C.

The example demonstrates the effect of temperature assignment and its uncertainty on a routine ambient INP spectrum. It does not address aerosol sources or atmospheric processes, which will be examined in the separate study of the long-term dataset.

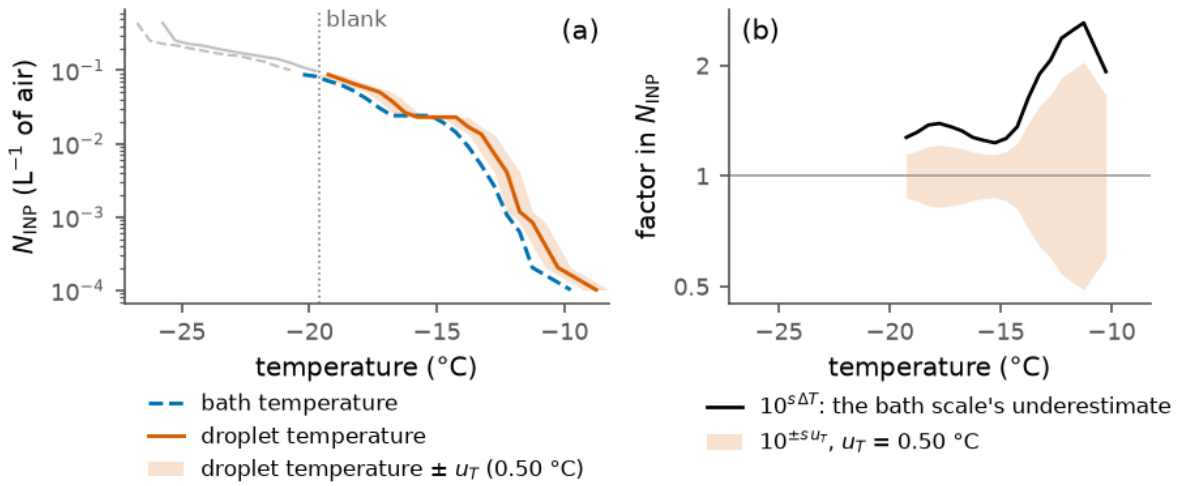


Figure R5. The ambient spectrum of the Pallas filter. (a) $N_{INP}(T)$ on the bath and the droplet temperature; grey, outside the useful range (dotted: the blank's warmest freezing event). (b) The resulting factors in concentration at a given temperature.

Changes in the revised manuscript.

A new application section shows the effect of the temperature assignment on an ambient INP spectrum (Fig. R5). Assigning the bath temperature instead of the droplet temperature would underestimate the concentration by a factor of 1.4 (median), larger than the factor of 1.2 that corresponds to the remaining temperature uncertainty. The intercomparison with GRAINS (RC1-3) and the cooling-rate comparison (RC2-7) are presented as further uses of the characterisation.

Reply to Referee #2

> *Perez Fogwill & Welti (2026) present a description of the droplet-freezing assay FrESH with a focus on the systematic temperature-uncertainty characterization. They decompose the total temperature uncertainty into the contributions from temporal resolution, bath-probe uncertainty, the static bath-well relationship, position-dependent variability, and dynamic effects during cooling ramps. This is done in a methodologically sound way, but without any innovation. The mechanical design of FrESH, with the floating PCR plate holder frame, is however a small but novel design choice, which mitigates fill-level issues that similar freezing assays might have. Overall, the manuscript does not have many weak points and is a solid characterization of the droplet-freezing assay, but it also does not bring innovation and novelty to the table of droplet-freezing assays. Since the scope of AMT does not explicitly demand novelty, I see no reason to reject the manuscript and hence recommend it for publication after revisions.*

We thank the referee for the detailed assessment and for noting the floating plate frame as a design feature. We reply to the individual comments below, numbered RC2-1 to RC2-7.

RC2-1: Section 3.2

> *At the end of 3.2. you mention the biggest weak point of your applied approach (thermal and non-thermal contributions cannot be separated).*

We agree. Referee #1 raised the same concern (RC1-2).

What we did and why.

We carried out the two experiments described in our reply to Referee #1 (RC1-2; Table R2 and Fig. R2). Plates frozen repeatedly and rotated or transferred between positions show whether a droplet's assigned freezing temperature follows the droplet or its position in the instrument. PT100 sensors in selected wells test whether the position-dependent freezing differences correspond to measured differences in well temperature.

What we found.

Instrument position accounts for part of the c_i field: rotated and transferred droplets changed their assigned freezing temperatures in the direction the field predicts, by about 0.3 to 0.8 of its magnitude for the three sample plates, with no detectable effect for the water blank (Table R3, Fig. R3a). The measured temperature differences between wells have the expected sign but are about a third of those the field predicts (slopes of 0.29 and 0.39 for the two chillers, where 1 would mean agreement; Fig. R3b). The remainder cannot be attributed with these measurements. On the RE1050 it follows the position rather than the droplets, so it is not an effect of the filling order; it may include temperature effects not captured by the sensors or optical detection effects (RC1-2).

Changes in the revised manuscript.

We agree, and Sect. 3.2 now states this limitation explicitly. The two new experiments (RC1-2) address it in part: instrument position accounts for part of the c_i field, and about a third of the field corresponds to measured temperature differences between wells, while the remainder cannot be attributed with these measurements. The spatial term is therefore retained as an

operational contribution to the uncertainty of the assigned freezing temperature, not as a measured temperature difference.

RC2-2: number and positions of the PT100 sensors

> *It is not clear to me why more PT100s were not simply used. If there is a valid reason it should be mentioned.*
> *Also, if you are limited to five sensors for whatever reason, could you not have randomized the PT100 positions across several runs? That could provide a full picture of the temperature distribution with actual temperature measurements instead of the more indirect approach using freezing statistics. Since the spatial uncertainty was identified as the largest or second-largest source of uncertainty (depending on chiller model), the authors should try to address and characterize this uncertainty as best as possible.*

The original five-sensor arrangement was intended to determine the average bath-to-well relationship, not to map the full temperature distribution. The number of sensors is limited in practice: each PT100 needs its own read-out channel (a MAX31865 converter) and its own intercalibration before use, and its leads have to be routed onto the floating plate frame. Each lead adds weight and tension to the frame and can change how deep it sits in the bath, which is what the frame is designed to keep constant. Following the referee's suggestion, we relocated the existing sensors between runs to increase spatial coverage.

What we did and why.

One sensor was kept in well A6 of plate position A as a reference. The other four were moved between selected edge and interior wells, two in each plate position, over 14 runs at $1\,^{\circ}\mathrm{C\,min^{-1}}$ (8 on the RE1050 and 6 on the RP1845), covering 36 wells (Fig. R2). The original five-sensor arrangement was repeated on both chillers (once on the RE1050, twice on the RP1845).

We selected positions rather than randomising them, to test the observed c_i field directly. They included wells with contrasting c_i values, positions along the main spatial gradient, interior wells, and pairs exchanged by a 180° rotation. Because the selection includes extremes of the field, the spread of these measurements alone is not used to estimate plate-wide spatial variability. Some wells were measured again in later runs with other sensors, after removal and reinsertion, to assess sensitivity to placement.

What we found.

The measured temperature differences had the sign expected from c_i, but were about a third of the predicted contrasts (Fig. R3b; see also RC1-2). These measurements extend the direct spatial coverage, but they do not provide a temperature map of all 96 wells over the full operating range.

We also corrected the description of the original sensor positions: all five were in edge wells. A6 had incorrectly been described as sampling a central region. Relative to the edge wells, the interior wells measured were on average 0.05 (RE1050) and 0.12 °C (RP1845) warmer, after removing the run offsets, which is small compared with the combined uncertainty; the average relation from edge wells is therefore not markedly biased with respect to the interior.

Changes in the revised manuscript.

Sect. 2.2 now explains why the number of sensors is limited (each needs its own read-out

channel, and its leads load the floating plate frame) and states the purpose and positions of the original sensors: "Five PT100 sensors, in wells H1, H12 and A6 of plate position A and A1 and A12 of plate position B, were used to determine the average relation between bath and well temperature; they do not map the temperature distribution across the plate." Following the referee's suggestion, a new Methods subsection describes how the sensors were relocated between runs, covering 36 wells in 14 runs, and why the positions were selected rather than randomised (Fig. R2); the Results compare these measurements with the c_i field (RC1-2).

RC2-3: samples and filling order

> *What samples were used to derive the freezing statistics? Did you, and if so how, ensure that the sample suspension was homogeneous? Did you fill the PCR plates in an ordered manner or randomly? Depending on your procedure, it might be possible, for example, that certain particles separate in the pipette through gravitational settling, so that the first drops contain more of certain particles, which in turn affects the spatial freezing pattern if the first drops are always placed, e.g., in the top left corner of a PCR plate.*

The freezing statistics come from the routine plates of daily ambient filters collected at Pallas, Kuopio and Utö: 1694 plates measured in 2025, all prepared with the same FrESH protocol. The long-term dataset they belong to will be published separately. The plates are filled in a fixed order, so a filling effect would appear at fixed positions; we estimated the settling of particles during the procedure and looked for a filling pattern in the routine data.

What we did and why.

Protocol. Each filter is placed in a 15 mL tube with 10 mL of filtered Milli-Q water and vortexed for 30 s; the tube is shaken again by hand immediately before pipetting. The plate is filled with an electronic pipette (Sartorius Picus, 1000 µL), which takes up 1 mL and dispenses 20 droplets of 50 µL. The wells are filled in a serpentine order starting at row A, the same in every plate, and the plates are always placed in the same orientation. No more than 10 min pass between placing the filter in the tube and placing the plate in the chiller.

Settling. We estimated with Stokes' law how far particles settle within one pipette load (about 1 min) and over the whole procedure (Fig. R6).

Filling pattern. Settling in the pipette tip would make the first droplets of every load differ from the last, a pattern that repeats every 20 wells and has the same sign in all four plate positions. We looked for it in the routine c_i field.

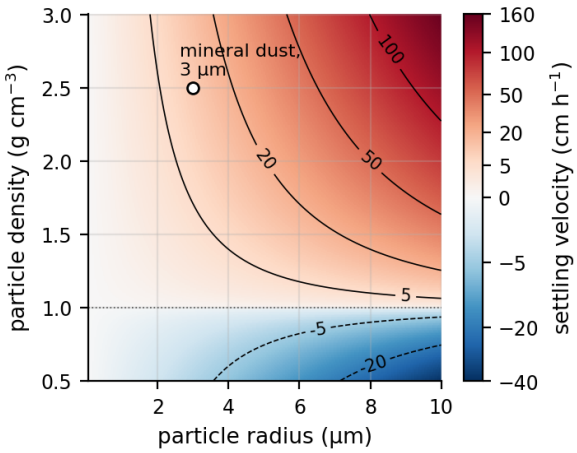


Figure R6. Density and size dependent sinking velocity of particles suspended in water, calculated using Stokes law.

What we found.

Within one pipette load, a mineral-dust particle (2.5 g cm^{-3}) of 3 µm radius settles about 2 mm, small compared with the liquid column in the tip; biological particles settle about ten times less (Fig. R6). Only coarse mineral particles, with radii above a few micrometres, settle appreciably over the whole procedure, and the tube is shaken again just before pipetting.

The routine c_i field shows no such pattern: the difference between the wells filled by the last and by the first five droplets of a load is -0.31 to 0.16 °C in the four plate positions, without a common sign. Because the filling order and the plate orientation are the same in every routine plate, a small common filling contribution cannot be separated from position in the routine data, and we keep it as a limitation of the spatial term (RC1-2). In the fixed plates the rotation does separate them: an effect of the filling order travels with the droplet, and for P1 the rotation leaves room for at most about a third of the rotation-sensitive part of the field to do so (RC1-2).

Changes in the revised manuscript.

Sect. 2 now describes the samples behind the freezing statistics (the routine plates of daily ambient filters), how the suspensions are mixed, and the filling protocol, including the fixed filling order and the time from preparation to measurement. Sect. 3.2 adds the settling estimate (Fig. R6), which shows that gravitational settling within a pipette load is negligible except for coarse mineral particles, and states that the routine field shows no filling pattern, but that a small common filling contribution cannot be separated from position in routine plates and may be included in the spatial term.

RC2-4: Fig. 2, larger spread at -25 °C and below

> *At bath temperatures of -25°C and below, there seems to be a larger step up in the 1σ range compared to the higher temperatures. Do the PT100 sensor readings get less accurate at $\leq$ -25°C, or is it another effect?*

The error bars in Fig. 2 show $\pm 1\sigma$ between sensors at different well positions, not the accuracy of the sensors. The larger spread at low temperature reflects temperature differences between well positions, which grow as the bath cools.

What we did and why.

We compared the five sensors in the stirred ethanol bath against a reference thermometer, from 0 to −35 °C. We tested whether freezing of the water around the sensors changes their readings, in ramps at 0.1 °C min^{-1}. We also examined the individual sensor records of the step runs behind Fig. 2.

What we found.

In the stirred bath, the between-sensor standard deviation, as logged before the intercalibration, did not exceed 0.07 °C at any setpoint. In the slow-ramp tests, the change associated with freezing was less than 0.1 °C on average.

In the step runs, all instrumented wells were warmer than the bath. The offsets increased from about 0.2–0.5 °C at 0 °C to about 0.8–2 °C at −35 °C, and largely the same positions were the warmest from run to run. The increasing separation between the sensor records is also reflected in the different slopes of the individual bath-to-well relations (Table A1).

These results support a position-dependent origin of the larger spread rather than an increase in disagreement between sensors at low temperature. They do not, however, establish a separate cause for the sharper increase below about −20 °C.

Changes in the revised manuscript.

The PT100 readings do not become less accurate at low temperature: in the stirred bath, the sensors agreed within 0.07 °C (one standard deviation) down to −35 °C. The Fig. 2 caption now states that the error bars show the spread between sensors at different well positions, not the accuracy of the sensors, and Sect. 2.2 describes the sensor checks. Sect. 4.1 attributes the larger spread at low temperature to temperature differences between well positions that grow as the bath cools, and notes that the sharper increase below about −20 °C has no separate explanation.

RC2-5: Section 4.3, combination in quadrature

> *You combine the uncertainty terms in quadrature, which implies that you see them as uncorrelated signals, but the dynamic and spatial terms, for example, likely share a common cause (bath circulation/heat transfer), which could mean some double-counting or under-counting of correlated error. How do you justify combining the terms in quadrature?*

We agree that independence was not established in the submitted manuscript. Both the spatial and the dynamic term may be affected by bath circulation and heat transfer. The dynamic term describes how each probe's temperature varies about its own mean during the ramp, and the spatial term the persistent differences between well positions, derived from the routine freezing statistics. A common cause does not by itself establish correlation. We therefore examined whether the differences between positions change with cooling rate, as a test of a possible dynamic contribution to the spatial pattern.

What we did and why.

We repeated measurements at slower cooling rates with the same sensors in the same wells (one run per chiller at 1 and 0.1 °C min^{-1}) and with the fixed plates (P1 and P1_D10 at their home positions at 0.05, 0.1 and 0.3 °C min^{-1}, and P2 in plate position B of the RE1050 at 0.1 °C min^{-1}). If the differences between positions were independent of the ramp, they would not change

with the cooling rate. We also recalculated the combined uncertainty assuming perfect positive correlation between the spatial and dynamic terms, adding these two terms linearly before combining them in quadrature with the remaining terms (Table R4).

What we found.

The differences between positions depend on the cooling rate. At 0.1 °C min^{-1}, the temperature contrast between the sensors' wells was about two thirds of that at 1 °C min^{-1} on both chillers. In the fixed plates, droplets at slower rates changed against the c_i field: part of the position pattern seen at 1 °C min^{-1} disappears in slower ramps. The spatial and dynamic contributions may therefore share physical influences, but these measurements do not quantify their covariance.

We therefore present the quadrature sum as a working assumption of zero covariance, not as a demonstrated independence of the two contributions. With $u_T^2 = \sum_i u_i^2 + 2\rho\, u_{\text{spatial}} u_{\text{dynamic}}$ and the revised spatial term (RC1-2), zero covariance ($\rho = 0$) gives 0.50 °C for the RE1050 and 0.44 °C for the RP1845, and perfect positive correlation ($\rho = 1$, the two terms added linearly) gives 0.69 and 0.59 °C (Table R4). These values show the sensitivity of the budget to the assumed covariance; they do not establish strict bounds on the total uncertainty. We retain the quadrature sum as the main operational estimate, while explicitly acknowledging the uncertainty associated with the unknown covariance.

The submitted budget also omits the calibration of the PT100 sensors against the reference thermometer. Each sensor was adjusted to the reference with a single constant offset; sensors adjusted this way read on average 0.1 to 0.2 °C above the reference at −15 °C and below, all in the same direction. This error is common to both chillers and to all wells, so it does not affect the comparisons between positions or chillers, but it shifts every corrected temperature. The revised budget includes it as a separate term; the values of u_T given in this reply do not yet include it.

Table R4. Uncertainty budget (Table 2) as submitted and with the spatial term from the revised field. Last row: the spatial and dynamic terms added linearly and the result combined in quadrature with the other terms.

	RE1050 (°C)		RP1845 (°C)	
Term	Submitted	Revised	Submitted	Revised
Temporal, u_{temporal}	0.08	0.08	0.08	0.08
Bath probe, u_{BT}	0.02	0.02	0.02	0.02
Model fit, u_{model}	0.11	0.11	0.11	0.11
Spatial, u_{spatial}	0.26	0.36	0.36	0.36
Dynamic, u_{dynamic}	0.32	0.32	0.21	0.21
Combined in quadrature, u_T	0.43	0.50	0.44	0.44
Spatial and dynamic added linearly	0.60	0.69	0.59	0.59

Changes in the revised manuscript.

Sect. 4.3 now states that the combination in quadrature assumes zero covariance between the terms, which our measurements cannot establish, and Table 2 adds the sensitivity case of perfect positive correlation between the spatial and dynamic terms, which raises the combined uncertainty from 0.50 and 0.44 °C to 0.69 and 0.59 °C (Table R4). The Results report the slower-rate measurements, which show that part of the spatial pattern depends on the cooling rate,

and the budget adds a term for the calibration of the PT100 sensors against the reference thermometer (Sect. 2.2).

RC2-6: chiller-specific values

> *The authors show that there are consistent temperature bias patterns within one PCR plate and also from plate to plate. However, in the end, they seem to plan on using chiller-model-specific values for the uncertainty and for the correction of the bath-well offset. Can you explain your reasoning behind this?*

The values are specific to each of our two chillers, one unit of each model, and to the plate-holder configuration used here. They are not calibration values for the chiller model; another instrument would require its own characterisation. We will state this explicitly.

The correction and the spatial term serve different purposes. The correction is the average bath-to-well relation measured with the PT100 sensors in each chiller. We do not correct individual wells because the routine freezing pattern is not a direct temperature map. The PT100 measurements cover only selected wells and do not fully reproduce the contrasts inferred from the freezing statistics (RC1-2).

The spatial term accounts for unresolved position-dependent variability. For each chiller, we use the larger of the values obtained for its two plate positions, rather than averaging them.

What we did.

We measured the same droplets of three fixed plates (P1, P2 and P1_D10; the blank was left out because its freezing temperatures drift) in both plate positions of both chillers, and fitted one temperature offset per plate position to all their runs.

What we found.

Within each chiller, the fitted offsets for the two plate positions differed by less than 0.1 °C. We therefore retain one average correction per chiller rather than separate corrections for the two plate positions.

After applying the respective chiller corrections, the freezing temperatures of the same droplets still differed by about 0.3 °C between chillers, consistently across plates and plate positions. This difference is smaller than the uncertainty of a corrected temperature on either chiller, but our data do not resolve its cause. It does not arise from the calibration of the PT100 sensors against the reference thermometer: the same sensors, in the same wells, characterised both chillers in alternating runs, so an error in their calibration shifts both corrections equally and cancels in this comparison. The revised manuscript reports it as an observed difference between the two chillers.

The conclusions were unchanged when the analysis was restricted to measurements made before the droplets' freezing pattern stopped reproducing after repeated freeze–thaw cycles (P1 then has valid data in only two of the four plate positions).

Changes in the revised manuscript.

Sect. 3.3 now states that the correction and the uncertainty apply to the two characterised units and their plate-holder configuration, not to a chiller model, and explains why one average correction is used per chiller while the spatial term takes the larger of its two plate positions.

The Results report the test with the same droplets in all four plate positions, which supports one correction per chiller (the two plate positions of a chiller agree within 0.1 °C) and shows a remaining difference of about 0.3 °C between the chillers.

RC2-7: further recommendation, cooling rates

> *As mentioned in my introduction, I am missing innovative and new aspects in the presented manuscript. One aspect that could be explored is different cooling rates and the effects of chiller-specific parameters like cooling capacity and pump flow. For cold-stage-based freezing assays, the effect of different freezing rates was investigated by, e.g., Jakobsson et al. (2022); for freezing assays using PCR plates, different cooling rates are largely unexplored.*

FrESH allows different programmed cooling rates. We have added an initial comparison, while retaining 1 °C min^{-1} as the operating condition characterised in this study. Both baths follow this rate down to about −20 °C; below, they cool more slowly as they approach their cooling capacity, at 0.86–0.97 °C min^{-1} between −20 and −25 °C and 0.45–0.50 °C min^{-1} near −35 °C. The characterisation therefore applies to the rates the baths actually follow under a programmed 1 °C min^{-1}.

What we did.

Two fixed plates (P1 and P1_D10, at their home positions) were measured at programmed cooling rates of 0.3, 0.1 and 0.05 °C min^{-1}, and a third (P2, in plate position B) at 0.1 °C min^{-1}, all on the RE1050, across three sessions. These measurements were interleaved with cycles at 1 °C min^{-1} using the same droplets (Fig. R7). The pump setting was not changed.

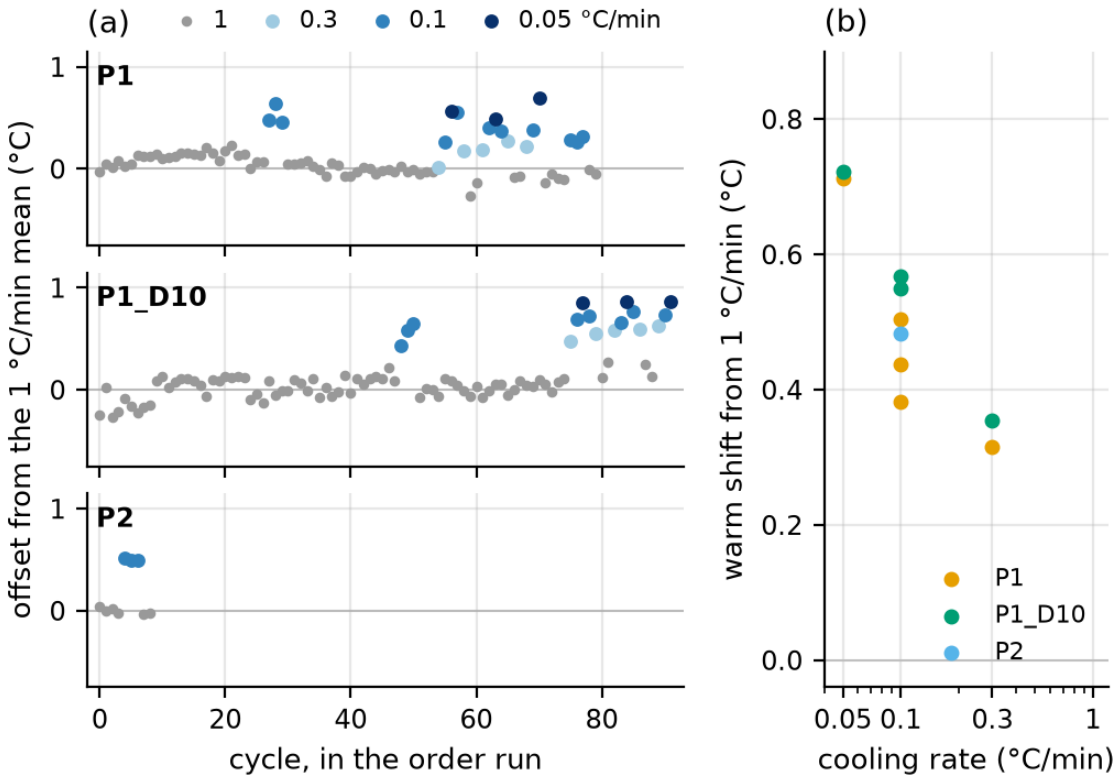


Figure R7. (a) Offset of each fixed plate in every cycle (median droplet minus its mean at 1 °C min^{-1}), in the order measured, coloured by cooling rate. (b) Warm shift from 1 °C min^{-1} in each session.

What we found.

In each session, slower cooling shifted freezing towards warmer temperatures. Relative to 1 °C min^{-1}, the shifts were approximately 0.3 °C at 0.3 °C min^{-1}, 0.4–0.6 °C at 0.1 °C min^{-1}, and 0.7 °C at 0.05 °C min^{-1}. In these tests, this corresponds to approximately 0.5 °C per tenfold decrease in cooling rate.

The shift of the plate median is not explained by a change in the average bath-to-well offset: on the RE1050, the PT100 measurements showed a change of less than 0.1 °C between 1 and 0.1 °C min^{-1}, although the contrasts between wells do depend on the rate (RC2-5).

The direction of the shift is consistent with the time dependence of ice nucleation (Herbert et al., 2014; Jakobsson et al., 2022). However, these plates had undergone many freeze–thaw cycles, and only a few cycles were measured at each slower rate. We therefore report this as an initial cooling-rate comparison, not a full characterisation or a separation of stochastic and instrumental contributions.

Changes in the revised manuscript.

Sect. 2.1 now reports the cooling capacity of the two chillers and the rates the baths actually follow: the programmed 1 °C min^{-1} down to about −20 °C, and about 0.5 °C min^{-1} near −35 °C. A new section presents the cooling-rate comparison with the fixed plates (Fig. R7): slower cooling shifts freezing to warmer temperatures by about 0.5 °C per tenfold decrease in rate, consistent with the time dependence of ice nucleation and not explained by a change in the bath-to-well offset. It is reported as an initial comparison for these plates and conditions, with the pump setting unchanged, not as a general correction.

References

Bazo, E., Ruiz-Galera, O., Alados-Arboledas, L., Böhmländer, A., Höhler, K., Kim, N., Lacher, L., Möhler, O., Olmo, F. J., Perez Fogwill, G., Piedehierro, A. A., Umo, N. S., Welti, A., Titos, G., and Cazorla, A.: Evaluation of different sampling methods to determine the ice-nucleating particle concentration in the atmosphere using the GRAnada Ice Nuclei Spectrometer (GRAINS), Atmos. Meas. Tech., 19, 2695–2713, https://doi.org/10.5194/amt-19-2695-2026, 2026.

David, R. O., Cascajo-Castresana, M., Brennan, K. P., Rösch, M., Els, N., Werz, J., Weichlinger, V., Boynton, L. S., Bogler, S., Borduas-Dedekind, N., Marcolli, C., and Kanji, Z. A.: Development of the DRoplet Ice Nuclei Counter Zurich (DRINCZ): validation and application to field-collected snow samples, Atmos. Meas. Tech., 12, 6865–6888, https://doi.org/10.5194/amt-12-6865-2019, 2019.

Herbert, R. J., Murray, B. J., Whale, T. F., Dobbie, S. J., and Atkinson, J. D.: Representing time-dependent freezing behaviour in immersion mode ice nucleation, Atmos. Chem. Phys., 14, 8501–8520, https://doi.org/10.5194/acp-14-8501-2014, 2014.

Jakobsson, K. F., Waman, D. B., Phillips, V. T. J., and Bjerring Kristensen, T.: Time dependence of heterogeneous ice nucleation by ambient aerosols: laboratory observations and a formulation for models, Atmos. Chem. Phys., 22, 6717–6748, https://doi.org/10.5194/acp-22-6717-2022, 2022.

Kunert, A. T., Lamneck, M., Helleis, F., Pöschl, U., Pöhlker, M. L., and Fröhlich-Nowoisky, J.: Twin-plate Ice Nucleation Assay (TINA) with infrared detection for high-throughput droplet freezing experiments with biological ice nuclei in laboratory and field samples, Atmos. Meas. Tech., 11, 6327–6337, https://doi.org/10.5194/amt-11-6327-2018, 2018.

Miller, A. J., Brennan, K. P., Mignani, C., Wieder, J., David, R. O., and Borduas-Dedekind, N.: Development of the drop Freezing Ice Nuclei Counter (FINC), intercomparison of droplet freezing techniques, and use of soluble lignin as an atmospheric ice nucleation standard, Atmos. Meas. Tech., 14, 3131–3151, https://doi.org/10.5194/amt-14-3131-2021, 2021.

Schrod, J. and Bingemer, H. G.: A view on recent ice-nucleating particle intercomparison studies: why the uncertainty of the activation temperature matters, Atmos. Meas. Tech., 18, 2591–2605, https://doi.org/10.5194/amt-18-2591-2025, 2025.

Wang, K., Bi, K., Chen, S., Hartmann, M., Wu, Z., Gao, J., Xu, X., Cheng, Y., Huang, M., Chen, Y., Xue, H., Wang, B., Hu, Y., Zhang, X., Ma, X., Li, R., Tian, P., Möhler, O., Wex, H., Stratmann, F., Chen, J., and Gong, X.: An improved Freezing Ice Nucleation Detection Analyzer (FINDA) for droplet immersion freezing measurement, Atmos. Meas. Tech., 18, 5823–5840, https://doi.org/10.5194/amt-18-5823-2025, 2025.

Wieber, C., Rosenhøj Jeppesen, M., Finster, K., Melvad, C., and Šantl Temkiv, T.: Micro-PINGUIN: microtiter-plate-based instrument for ice nucleation detection in gallium with an infrared camera, Atmos. Meas. Tech., 17, 2707–2719, https://doi.org/10.5194/amt-17-2707-2024, 2024.